Chem. Senses 35: 511–521, 2010
doi:10.1093/chemse/bjq043
Advance Access publication May 9, 2010

Arrangement of Output Information from the 3 Macroglomerular Units in the Heliothine Moth *Helicoverpa assulta:* Morphological and Physiological Features of Male-Specific Projection Neurons

Xin-Cheng Zhao and Bente G. Berg

Department of Psychology and Neuroscience Unit, Medical Technical Research Center (MTFS), Norwegian University of Science and Technology, Olav Kyrres gate 9, N-7489 Trondheim, Norway

Correspondence to be sent to: Bente G. Berg, Department of Psychology and Neuroscience Unit, MTFS, Norwegian University of Science and Technology, Olav Kyrres gate 9, N-7489 Trondheim, Norway. e-mail: bente.berg@ntnu.no

Accepted April 12, 2010

Abstract

Helicoverpa assulta is exceptional among heliothine species studied so far as concerns composition of the pheromone blend. Previous reports have accordingly pointed out distinct characteristics in the male-specific olfactory pathway of this species, peripherally by an unusual distribution of 2 sensillum categories and centrally by a particular anatomical arrangement of the male-specific glomeruli constituting the macroglomerular complex (MGC). In order to determine the physiological tuning of the 3 MGC units in this species, we have characterized male-specific antennal-lobe projection neurons morphologically and physiologically by use of the intracellular recording and staining technique combined with confocal microscopy. The results show 2 projection neuron types of equal numbers, one that responds to the primary pheromone component, *cis*-9-hexadecenal, and arborizes in the cumulus and one that responds to the interspecific signal, *cis*-9-tetradecenal, and arborizes in the dorsomedial unit. A third type responded to the secondary pheromone component, *cis*-11-hexadecenal, and innervated the smaller ventral unit. The results complement previous findings from tracing of physiologically identified receptor neurons and determine for the first time the functional specificity of each glomerulus in the MGC of *H. assulta*. The results are particularly interesting because heliothine moths are attractive objects for comparative studies addressing questions concerning divergence of male-specific olfactory characteristics related to speciation.

Key words: behavioral antagonist, evolutionary perspective, insect pheromone, intracellular recordings, odor coding, the oriental tobacco budworm moth

Introduction

The antennal lobe is the primary olfactory center of the insect brain. Like its analog in the vertebrate brain, the olfactory bulb, this processing region consists of numerous spherical structures termed glomeruli that are synaptic neuropil of sensory axon terminals making contact with second-order neurons, that means local interneurons and projection neurons (Hildebrand and Shepherd 1997; Anton and Homberg 1999). Thus, the odor signals are detected by the receptor neurons and conveyed as nerve impulses to the glomeruli. Here, the input information is processed by the local network before being sent by projection neurons to higher integration centers of the brain (Boeckh and Ernst 1987; Christensen and Hildebrand 1987; Homberg et al. 1988; Ng et al. 2002; Wilson et al. 2004; Root et al. 2007). In male moths, a considerable number of receptor neurons target a group of enlarged glomeruli located dorsally in the antennal lobe at the entrance of the antennal nerve. It is well documented that this arrangement of sexually dimorphic glomeruli, known as the macroglomerular complex (MGC), is dedicated to processing information about female-produced pheromones for the purpose of reproductive behavior (Christensen and Hildebrand 1987; Hansson et al. 1991, 1992, 1994; Mustaparta 1996; Anton et al. 1997; Kanzaki et al. 2003).

Species of the monophyletic group *Heliothinae* utilize pheromone blends made up of partial similar constituents, however, in a species-specific composition (cf. Arn et al. 1992). These noctuid moths, that comprise more than 80 species distributed in all 5 continents, have therefore been attractive objects for comparative studies addressing questions concerning divergence of male-specific chemosensory hallmarks related to

speciation. By tracing of functionally characterized receptor neurons and antennal-lobe projection neurons, a general chemotopic organization of the MGC has been demonstrated in a number of allopatric (i.e., geographically isolated) and sympatric species of the 2 genera *Heliothis* and *Helicoverpa*, including *Heliothis virescens* (Christensen et al. 1995; Hansson et al. 1995; Berg et al. 1998; Vickers et al. 1998; Vickers and Christensen 2003), *Heliothis subflexa* (Baker et al. 2004; Lee, Vickers, and Baker 2006), *Helicoverpa zea* (Christensen et al. 1991; Cossé et al. 1998; Vickers et al. 1998; Lee, Carlsson, et al. 2006), *Helicoverpa assulta* (Berg et al. 2005), and *Helicoverpa armigera* (Skiri 1999). Particularly interesting is the fact that the MGC of heliothine species have established 2 parallel pathways—one for pheromone information underlying attraction and sexual behavior and one for signal information emitted from heterospecifics ensuring reproductive isolation. Thus, in addition to MGC units receiving input about pheromone constituents, particular glomeruli serve as target areas of receptor neurons tuned to a substance that is absent from the pheromone blend of the conspecific female but present in the blend of a sympatric heterospecific female (Christensen et al. 1995; Mustaparta 1996; Vickers et al. 1998; Berg et al. 2005).

Among the heliothine species mentioned above, the oriental tobacco budworm moth, *H. assulta*, is exceptional as concerns composition of the pheromone blend. Whereas the other species rely on *cis*-11-hexadecenal (Z11-16:AL) as the major pheromone component, *H. assulta* uses this substance as the secondary component and *cis*-9-hexadecenal (Z9-16:AL) as the primary one (Sugie et al. 1991; Cork et al. 1992; Park et al. 1994). Consequently, a large number of male-specific receptor neurons tuned to Z9-16:AL and a small number tuned to Z11-16:AL have been identified in *H. assulta* (Berg and Mustaparta 1995). A third neuron category consistently colocalized with the most numerous pheromone neuron type is tuned to *cis*-9-tetradecenal (Z9-14:AL; Berg and Mustaparta 1995), a behavioral inhibitor (Boo et al. 1995). The closely related congeners *H. armigera* and *H. zea* also utilize a binary pheromone blend consisting of Z9-16:AL and Z11-16:AL—the 2 constituents existing in an opposite ratio to that of *H. assulta* (Klun et al. 1980; Wang et al. 2005). The cotton budworm *H. armigera* is sympatric with *H. assulta*, both belonging to the so-called Old World species, whereas the allopatric corn earworm *H. zea* belongs to the New World species. Previous anatomical studies have revealed a 3-unit MGC in all 3 species of the *Helicoverpa* genus, one prominent unit situated at the antennal nerve entrance, the so-called cumulus, and 2 additional units (Christensen et al. 1991; Vickers et al. 1998; Berg et al. 2002; Skiri et al. 2005). Different from *H. zea* and *H. armigera*, having the 2 additional units located dorsomedially of the cumulus, *H. assulta* has one dorsomedial and one ventral unit surrounding the cumulus (Figure 1). Thus, the unique pheromone blend of *H. assulta* seems to be mirrored in the anatomical organization of the MGC as well.

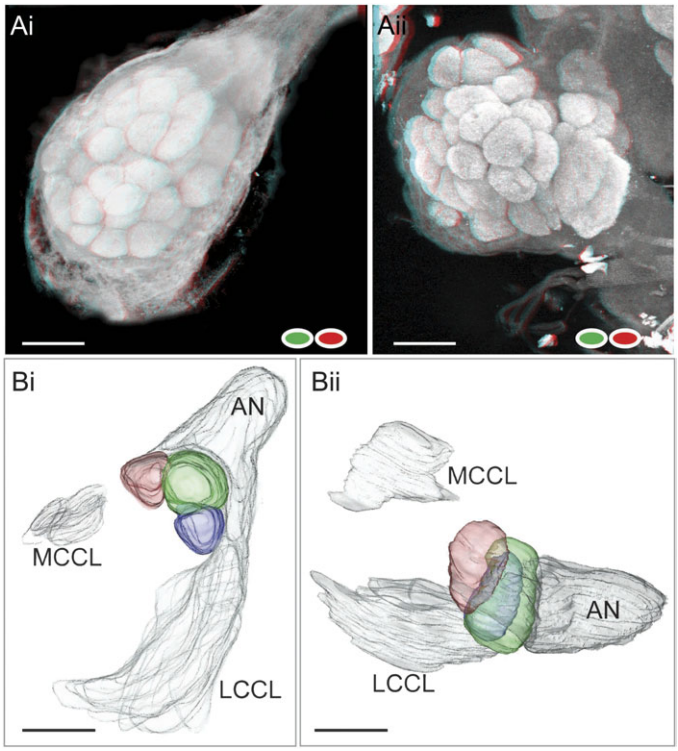

Figure 1 The antennal lobe (AL) of the *Helicoverpa assulta* male, showing the dorsally located MGC. **(A)** Stereo images of the AL in a frontal **(Ai)** and dorsal view **(Aii)** representing the glomeruli covering the surface of the antennal lobe. The cumulus and the dorsomedial MGC unit appear as enlarged glomeruli located at the entrance of the antennal nerve (AN), adjacent to the numerous ordinary glomeruli. (For stereo view, utilize red green 3D glasses.) **(B)** Digital reconstructions of the 3 MGC units in a frontal **(Bi)** and a dorsal view **(Bii)**. The cumulus (green) and the dorsomedial unit (red) are situated dorsally of the ventral unit (blue). The reconstructions were made from confocal images (Berg et al. 2002) by use of the AMIRA software. MCCL, medial cell cluster; LCCL, lateral cell cluster; Scale bars = 100 μm.

Furthermore, tracing of the physiologically characterized receptor neuron types has previously demonstrated a shift in the odor to which the cumulus is associated in *H. assulta* as compared with the other species; thus, in *H. armigera* and *H. zea*, as well as in species of the *Heliothis* genus, the cumulus receives input from receptor neurons tuned Z11-16:AL, here mediating information about the primary pheromone component (Hansson et al.1995; Berg et al. 1998; Vickers et al. 1998; Skiri 1999; Lee, Carlsson, et al. 2006; Lee, Vickers, and Baker 2006). However, in *H. assulta*, the receptor neurons tuned to Z11-16:AL project to the small ventral MGC unit, whereas the cumulus and the dorsomedial glomerulus each receives input from the 2 colocalized receptor neuron categories tuned to Z9-16:AL and Z9-14:AL (Berg et al. 2005). A pairing of the same receptor neuron types, one responding to Z9-16:AL and one to Z9-14:AL, has also been reported in *H. armigera* and *H. zea*—here targeting the 2 smaller dorsomedial MGC units (Skiri 1999; Lee, Carlsson, et al. 2006). Due to the colocalization in all 3 species, these

neuron types were consequently stained together during the previous tip-recording and staining experiments (Skiri 1999; Berg et al. 2005; Lee, Carlsson, et al. 2006). As concerns *H. assulta*, it could therefore not be concluded which of the 2 neuron types projects in the cumulus and the dorsomedial unit, respectively.

From an evolutionary point of view, it is particularly interesting to compare the anatomical and functional organization of the 3-unit MGC across the *Helicoverpa* species. In the present study, we have characterized male-specific antennal-lobe projection neurons in *H. assulta* physiologically and morphologically by use of the intracellular recording and staining technique combined with laser scanning confocal microscopy. The results show 2 projection neuron categories of equal numbers, one Z9-16:AL–responding type innervating the cumulus and one Z9-14:AL–responding type innervating the dorsomedial unit. A third category included one projection neuron responding to Z11-16:AL and arborizing in the ventral unit. The data presented here indicate a physiological tuning of each glomerulus in the MGC of *H. assulta* and consequently provide distinct knowledge for interspecific comparison in an evolutionary perspective.

Materials and methods

Insects and preparation

Helicoverpa assulta pupae, originating from a laboratory culture, were kindly provided by Dr Jun-Feng Dong (Henan University of Science and Technology, Henan, China). Male and female pupae were separated and kept in climate chambers on reversed photoperiod 14:10 h light:dark at 22 °C. The adults were fed a 5% sucrose solution. Experiments were performed on adult males 2–5 days after ecdysis, as previously described by Zhao and Berg (2009). Thus, the moth was restrained inside a plastic tube with the head and antennae exposed. The head was immobilized with wax (Kerr Corporation, Romulus, MI), and the antennae lifted up by needles. The brain was exposed by opening the head capsule and removing the mouthparts, the muscle tissue, and major trachea. The sheath of the antennal lobe was removed by fine forceps in order to facilitate microelectrode insertion into the tissue. Once the head capsule was opened, the brain was supplied with Ringer's solution (in mM: 150 NaCl, 3 $CaCl_2$, 3 KCl, 25 sucrose, and 10 *N*-tris (hydroxymethyl)-methyl-2-amino-ethanesulfonic acid, pH 6.9). The whole preparation was positioned so that the antennal lobes were facing upward and the ipsilateral antenna of the recording site could be stimulated with odorants.

Intracellular recording and staining

The intracellular recordings from the antennal-lobe neurons were carried out as previously described (Zhao and Berg 2009). Recording electrodes were made by pulling glass capillaries (Borosilicate glass capillaries; Hilgenberg GmbH; outer diameter: 1 mm, inner diameter: 0.75 mm) on a horizontal puller (P97, Sutter Instruments). The tip was filled with a fluorescent dye (4% tetramethylrhodamine dextran with biotin, Micro-Ruby, Molecular Probes; Invitrogen, in 0.2 M K^+-acetate), and the glass capillary backfilled with 0.2 M K^+-acetate. A chloridized silver wire inserted into the eye served as the indifferent electrode. The recording electrode, which had a resistance of 150–400 MΩ, was lowered carefully into the brain by means of a micromanipulator (Leica). The recording site was randomly chosen within the dorsal region of the antennal lobe, that means in the area of the MGC. Neuronal spike activity was, after being amplified (AxoClamp 2B; Axon Instruments), monitored continuously by oscilloscope and loudspeaker. The recordings were stored by the Spike2 6.02 software (Cambridge Electronic Design). In a few recordings resulting in more than one stained neuron, we have presumed that the electrophysiological signals originated from the neuron most heavily stained.

After physiological characterization according to odor stimuli, the neurons were iontophoretically stained by receiving 2–5 nA depolarizing current pulses with 200 ms duration at 1 Hz for about 2–10 min via the glass capillary electrode. In order to allow neuronal transportation of the dye, the preparation was kept for 1 h at room temperature. The brain was then dissected from the head capsule. After being fixed in 4% paraformaldehyde for 1 h at room temperature, the brain was rinsed with a phosphate-buffered saline (PBS; in mM: 684 NaCl, 13 KCl, 50.7 Na_2HPO_4, 5 KH_2PO_4, and pH 7.4). The staining was then intensified by incubating the brain in fluorescent conjugate streptavidin-Cy3 (Jackson Immunoresearch, diluted 1:200 in PBS), which binds to biotin, for 2 h. Incubation was followed by rinsing with PBS and dehydration in an ascending ethanol series (50%, 70%, 90%, 96%, and 2 × 100%; 10 min each). Finally, the brain was cleared and mounted in methylsalicylate.

Stimulation

The odor delivery system for the intracellular recording consisted of 2 glass cartridges placed side by side, both pointing toward the antenna at a distance of 2 cm. One replaceable cartridge contained a piece of filter paper onto which a particular odor stimulus was applied. The other cartridge contained a pure filter paper. An airflow (500 mL/min) led through one of the 2 cartridges was continuously blown over the antenna. During each stimulus period, which lasted for 400 ms, the airflow was switched by a valve system from the odorless to the odor-bearing cartridge.

Based on previous electrophysiological investigations that have identified ligands for the 3 types of male-specific receptor neurons and for a number of plant odor neuron types (Berg and Mustaparta 1995; Stranden et al. 2003), the following stimuli were used: the primary pheromone component Z9-16:AL, the secondary pheromone component Z11-16:AL, the interspecific signal Z9-14:AL, the binary

pheromone blend of Z9-16:AL and Z11-16:AL in the ratio 95:5 (all insect-produced substances delivered by Plant Research International, Pherobank, Wageningen, Netherlands), and the plant oil ylang-ylang (Dragoco). Because of the general difficulty of maintaining a stable contact between electrode and neuron in the tiny preparation, the collection of test compounds included only the most essential stimuli. Each compound, which was diluted in hexane, was applied onto a small filter paper. The hexane was allowed to evaporate before the filter paper was wrapped up and placed in the cartridge. All stimuli were prepared so that the filter paper contained a particular dose of each odorant, that is, 1 and 10 ng of each single insect-produced substance and of the binary pheromone blend and 100 μg of the plant oil. A cartridge containing a pure filter paper was used as control. The odor stimuli were regularly renewed during the experimental period.

Glomerular identification

In order to identify the 3 MGC units, immunostaining with a synapsin antibody marking synaptic structures was performed on each successfully labeled brain (data not shown). After having analyzed the iontophoretically stained neuron by confocal laser scanning microscopy, the brain was rehydrated through a decreased ethanol series (10 min each) and rinsed in PBS. To minimize nonspecific staining, the brain was submerged in 5% normal goat serum (NGS; Sigma) in PBS containing 0.5% Triton X-100 (PBSX; 0.1 M, pH 7.4) for 3 h at room temperature. The preparation was then incubated for 2 days at 4 °C in the primary antibodies, SYNORF1 and nc46 (dilution 1:10 and 1:40 in PBSX containing 5% NGS, respectively; SYNORF1 was delivered by Developmental Studies Hybridoma Bank, University of Iowa, and nc46 was kindly provided by Dr. E. Buchner, Würzburg, Germany). After being rinsed in PBS 6 × 20 min at room temperature, the brain was incubated with Cy2-conjugated antimouse secondary antibody (Invitrogen; dilution 1:500 in PBSX) for 2 days at 4 °C. Finally, after being rinsed again, the brain was dehydrated, cleared, and mounted in methylsalicylate.

Confocal microscopy, image processing, and data analyses

Serial optical images were acquired by using a confocal laser scanning microscope (LSM 510, META Zeiss) with a 40× objective (C-Achroplan 40×/0.8 W). The intracellular staining, obtained from the fluorescence of rhodamine/Cy3 (Ex_{max} 550 nm, Em_{max} 570 nm), was excited by the 543-nm line of a HeNe1 laser, and the synapsin immunostaining, obtained from the Cy2 (Ex_{max} 490 nm, Em_{max} 508 nm), was excited by the 488-nm line of a Argon laser. The distance between each section was 2 μm, the pinhole size 1, and the resolution 1024 × 1024 pixels. Optical sections from the confocal stacks were reconstructed by means of the LSM 510 projection tool. In order to adjust brightness and contrast, Adobe Photoshop CS2 (Adobe System) was used. The images were finally edited in Adobe Illustrator CS3.

The electrophysiological recordings were stored and analyzed by use of the Spike2 program. The responses were analyzed by counting the numbers of spikes within intervals of 100 ms during a total period of 5 s. The 5-s period started 1 s before stimulus onset and thus ended 3.6 s after stimulus offset. Based on the spike frequencies calculated, histograms that visualize the neuronal activity before, during, and after the stimulation period were made for each recording.

Results

Intracellular recordings performed from the antennal lobe of 69 males resulted in 14 physiologically characterized neurons (Table 1). They all responded to the insect-produced stimuli tested. Each of the recorded neurons was categorized according to the stimulus that elicited the strongest excitatory response. Two equally numbered types, each including 4 neurons, were tuned to the primary pheromone component Z9-16:AL and the interspecific signal Z9-14:AL, respectively. A third type, including one neuron, responded to the secondary pheromone component Z11-16:AL (Table 1, Figure 2). Due to the general instability of the recordings from the small brain preparation, not all stimuli were tested in each experiment. Ten of the neurons were successfully stained, all showing a principally similar morphology by being uniglomerular projection neurons with a cell body located in the medial cell cluster and an axon passing via the inner antennocerebral tract to the calyces of the mushroom bodies and the inferior lateral protocerebrum. One uniglomerular projection neuron (#14), innervating the ventral MGC unit, showed an excitatory response to the blank almost as strong as the response to the binary pheromone blend (Table 1). This neuron was not tested for any of the single insect-produced compounds.

Projection neurons responsive to Z9-16:AL

Based on an increased spike frequency to antennal stimulation with the primary pheromone component, 4 Z9-16:AL–responsive neurons (#1–4) were identified (Figures 2 and 3A). Stimulation with the binary pheromone blend evoked responses similar to those elicited by Z9-16:AL alone (Figure 3A). Three of the neurons (#1, #3, and #4) responded to Z9-16:AL only, whereas one neuron (#2) showed an additional inhibitory response to Z11-16:AL, ylang-ylang, and pure air during antennal stimulation with the single substances (Table 1, Figure 2).

Three of the 4 physiologically characterized neurons were labeled and they all innervated the cumulus. The dense dendritic arborizations of one of these uniglomerular projection neurons (#1) filling the large MGC unit is shown in Figure 3B,C. Due to incomplete staining, the protocerebral projections of this neuron could not be traced. The complete morphology of a Z9-16:AL–responsive output neuron is shown

Table 1 Summary of physiological and morphological characteristics of all encountered antennal-lobe neurons

Neuron	Z9-16:AL	Z9-14:AL	Z11-16:AL	Mixture	Ylang-ylang	Blank	Cell type	Location of PN soma	Tract of PN	Dendritic branches of PN	Axonal branches of PN
#1	+	0	0	+	nt	0	PN, LN	MCCL	IACT	C	ns
#2	+	0	–	+	–	–	PNs	MCCL	IACT	C	Ca, ILP
#3	+	0	0	+	0	0	PNs	MCCL	IACT	C, V	Ca, ILP
#4	+	0	0	nt	0	0	ns	ns	ns	ns	ns
#5	0	nt	+	nt	nt	0	PN	MCCL	IACT	V	Ca, ILP
#6	0	+	0	0	0	0	PN	MCCL	IACT	DM	Ca, ILP
#7	–	+	0	–	+	0	PN	MCCL	IACT	DM	ns
#8	0	+	0	0	0	0	PN	MCCL	IACT	DM	Ca, ILP
#9	nt	+	nt	0	0	0	PNs, LN	MCCL	IACT	DM	Ca, ILP
#10	nt	nt	nt	+	nt	0	ns	ns	ns	ns	ns
#11	nt	nt	nt	+	nt	0	PN	MCCL	IACT	C	Ca, ILP
#12	+	+	0	+	0	nt	ns	ns	ns	ns	ns
#13	nt	nt	nt	+	nt	0	ns	ns	ns	ns	ns
#14	nt	nt	nt	+	+	+	PN	MCCL	IACT	V	Ca, ILP

The physiological responses were defined as excitatory (+) or inhibitory (–) according to the changes of spike frequency. C, cumulus; DM, dorsomedial MGC unit; V, ventral MGC unit; IACT, inner antennocerebral tract; ILP, inferior lateral protocerebrum; LN, local interneuron; MCCL, medial cell cluster; Ca, calyces of the mushroom body; PN, projection neuron; S, soma; nt, not tested; ns, not stained.

in Figure 4 by 2 labeled neurons with similar projection patterns in the protocerebrum and overlapping arborizations in the cumulus (originating from the recording of neuron #2). One of the neurons sent off a few branches into a limited region of an ordinary glomerulus located nearby the somata (Figure 4D). The third labeled preparation, in which neuron #3 was recorded, showed a completely stained projection neuron displaying one axon passing in the inner tract to the calyces and the inferior lateral protocerebrum. The staining pattern in the antennal lobe, which included 2 labeled somata, showed dendritic arborizations in the cumulus and the ventral MGC unit (Table 1).

One successfully stained projection neuron (#11) excited by the binary pheromone blend arborized in the cumulus (Table 1). This neuron was not tested for any of the single insect-produced substances.

Projection neuron responsive to Z11-16:AL

One neuron (#5) responded to the secondary pheromone component Z11-16:AL. As shown in Figure 5A, an increased spike frequency appeared when Z11-16:AL was blown over the antenna. Stimulation with the primary pheromone component elicited no response; neither did stimulation with pure air. The interspecific signal Z9-14:AL and the binary pheromone mixture were not tested.

The morphology revealed a typical uniglomerular projection neuron with dense dendritic arborizations in the ventral MGC unit, an axon passing in the inner antennocerebral tract, and projection terminals in the calyces and the lateral inferior protocerebrum (Figure 5B–E). As demonstrated in Figure 5Bii,iii, the ventral MGC unit has the shape of a curved structure partially coiling the cumulus.

Projection neurons responsive to Z9-14:AL

Four neurons (#6–9) responded by an increased spike frequency to antennal stimulation with the interspecific signal Z9-14:AL (Figures 2 and 6A). None of the neurons displayed excitatory responses to the other insect-produced stimuli tested. One neuron (#7) showed an additional inhibitory response to Z9-16:AL and to the binary pheromone blend, as well as an excitatory response to ylang-ylang (Figure 2).

All 4 neurons were successfully stained and revealed uniglomerular projection neurons with arborizations in the dorsomedial MGC unit (Figures 6 and 7). With one exception (#7), their projections could be traced to the calyces and the lateral protocerebrum. In 2 preparations (neuron #8 and #9), a few faintly stained branches in some of the ordinary glomeruli appeared, probably belonging to local interneurons (Figure 7Bi,Ci).

Discussion

The results presented here demonstrate that each of the 3 MGC units in *H. assulta* houses the dendrites of a category

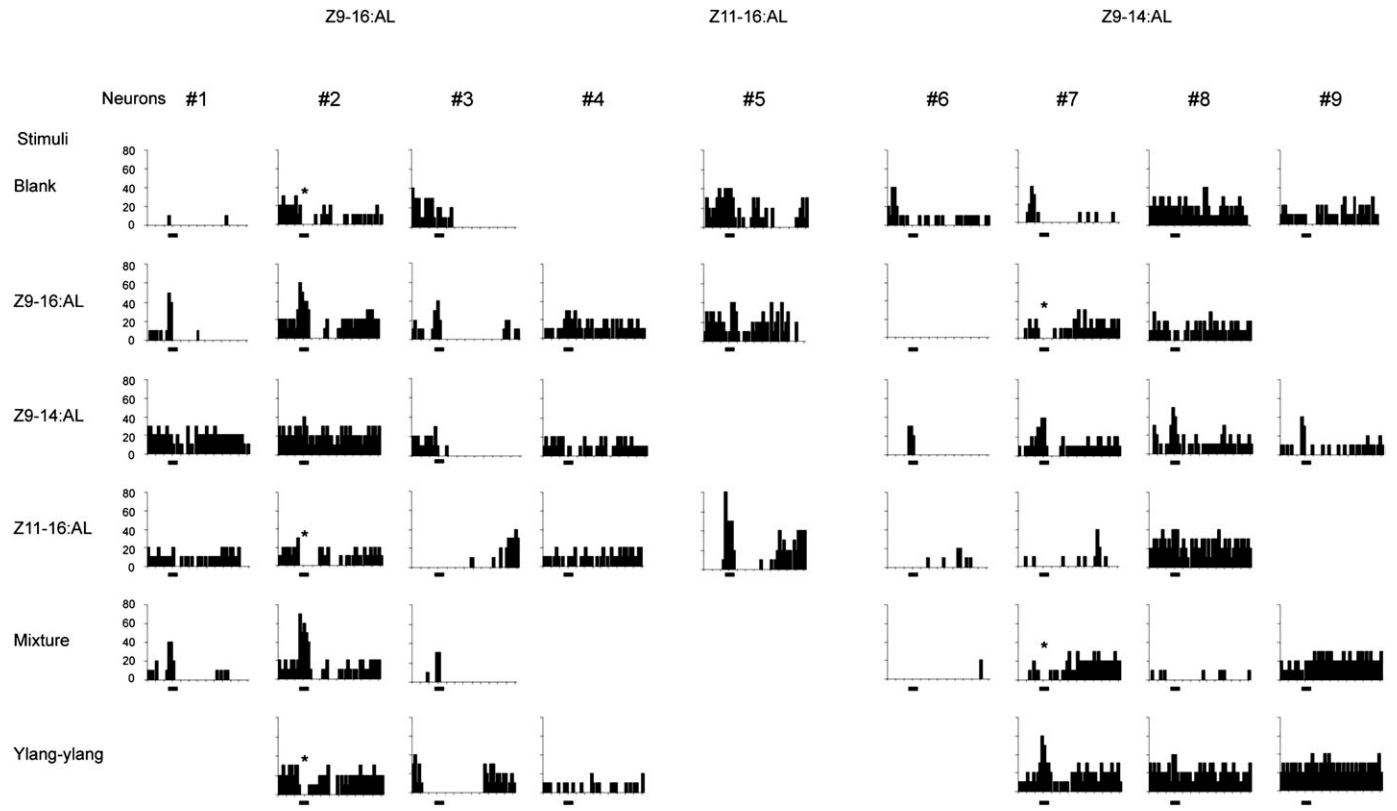

Figure 2 Histograms visualizing physiological characteristics of the 3 projection neuron categories identified, one selectively responsive to Z9-16:AL (neurons #1–4), one to Z11-16:AL (neuron #5), and one to Z9-14:AL (neurons #6–9). Each column represents the number of spikes counted during a period of 100 ms. Inhibitory responses are denoted by an asterisk. The concentrations of the insect-produced substances were 1 ng for neuron #4 and 10 ng for the others. The stimulation period (400 ms) is indicated below.

of uniglomerular projection neurons responding primarily to antennal stimulation with one of the binary pheromone components, Z9-16:AL or Z11-16:AL, or the interspecific signal Z9-14:AL. This kind of functional organization is in agreement with the projection pattern of receptor neurons previously reported in this species, including 3 receptor neuron types tuned to Z9-16:AL, Z11-16:AL, and Z9-14:AL, respectively (Berg et al. 2005). The close correspondence between input to and output from the different MGC units manifests the principle of chemotopy previously demonstrated in a number of other lepidopteran species (reviewed by Hansson and Christensen 1999).

Some of the projection neurons presented here, like neuron #2 and #7, showed in addition to an excitatory response to one particular compound an inhibitory response to some of the other stimuli (Figure 2). Such complex response profiles indicate that the uniglomerular projection neurons also integrate information from receptor neuron categories targeting adjacent glomeruli. Due to the relatively restricted number of successful recordings, the present data may well be an undersampling of the true variation characterizing the physiological and morphological properties of male-specific projection neurons. Previous publications have reported about uniglomerular projection neurons displaying synergistic responses to pheromone blends as well as multiglomerular neurons being narrowly tuned to one substance only (Christensen and Hildebrand 1987; Christensen et al. 1991, 1995; Hansson et al. 1991; Berg et al. 1998; Vickers and Christensen 2003; Kárpáti et al. 2008).

The cumulus is associated with the primary pheromone component Z9-16:AL

The present results which point out the cumulus as a dedicated site for processing information about Z9-16:AL in *H. assulta*, confirm a general principle that this MGC unit handles information about the primary pheromone compound in heliothine species, irrespective of the compound identity.

The response profiles of the Z9-16:AL specific projection neurons presented here, characterized by an excitatory response to the key compound only, differ from previous findings in the closely related congener *H. zea* where the population of projection neurons responding to Z9-16:AL was equally activated by Z9-14:AL (Christensen et al. 1991; Vickers et al. 1998). Projection neurons responding exclusively to Z9-16:AL have previously been identified in one heliothine species only, namely *H. subflexa* that belongs to the *Heliothis*

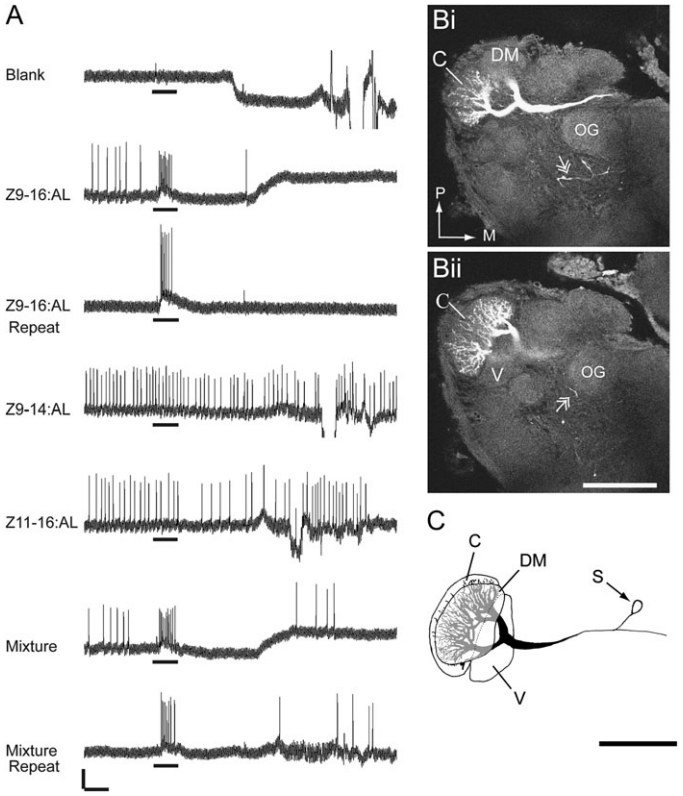

Figure 3 Physiological and morphological characteristics of a projection neuron responding to the primary pheromone component Z9-16:AL (neuron #1). **(A)** Neuronal activity recorded during application of various stimuli to the antenna. An excitatory response to Z9-16:AL and to the binary pheromone mixture is shown. (The shifts in membrane potential are mainly due to disturbance induced during removal of the odor-bearing cartridge from the stimulus setup.) Scale bars = 10 mV, 400 ms. **(Bi, Bii)** Two confocal sections at different depths (8 μm apart) showing an uniglomerular projection neuron with dense arborizations in the cumulus (C). Branches from a faintly stained local interneuron can be seen (double arrows). **(C)** Reconstruction of the dendritic arborizations restricted to the cumulus. Scale bars = 100 μm. DM, dorsomedial unit; V, ventral unit; OG, ordinary glomerulus; S, soma; P, posterior; M, medial.

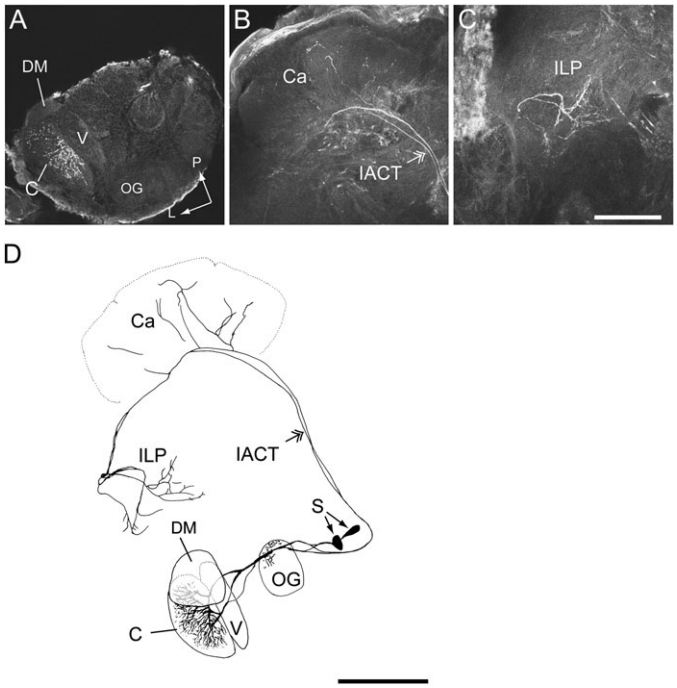

Figure 4 Complete morphology of 2 projection neurons with arborizations in the cumulus, one of which responded to Z9-16:AL (neuron #2). **(A–C)** Confocal sections showing the neural branches in the antennal lobe and the protocerebrum. Both neurons arborized in the cumulus **(A)** and projected via the inner antennocerebral tract (IACT; double arrow) to the calyces **(B)** and the inferior lateral protocerebrum **(C)**. **(D)** Complete reconstruction of the 2 neurons. Scale bars = 100 μm. C, cumulus; DM, dorsomedial unit; V, ventral unit; OG, ordinary glomerulus; Ca, Calyces; ILP, inferior lateral protocerebrum; S, somata; P, posterior; L, lateral.

genus (Vickers and Christensen 2003). The variations in response profiles of the Z9-16:AL–activated central neurons may reflect differences in specificities of the associated sensory neurons across the 3 species. Previous publications have reported that *H. assulta* and *H. subflexa* both possess a population of male-specific receptor neurons distinctively more sensitive to Z9-16:AL than to Z9-14:AL (Berg et al. 2005; Lee, Vickers, and Baker 2006), whereas *H. zea* has a population responding with approximately equal strength to the 2 substances (Cossé et al. 1998; Lee, Carlsson, et al. 2006).

Information about the behavioral antagonist Z9-14:AL is mediated by a large number of projection neurons arborizing in the dorsomedial MGC unit

The present finding of 2 equally numbered projection neuron categories tuned to the primary pheromone component Z9-16:AL and the interspecific signal Z9-14:AL, respectively, matches the composition of male-specific receptor neurons previously reported in *H. assulta* (Berg and Mustaparta 1995; Berg et al. 2005). The peripheral arrangement including a sensory neuron type tuned to an interspecific signal that is as numerous as the type tuned to the primary pheromone component therefore seems to be reflected in the antennocerebral pathways. Even though the colocalization of one antagonistically acting receptor neuron and one tuned to the major pheromone component has been reported in a number of moth species, as for instance *Trichoplusia ni*, *Agrotis segetum*, and *Ostrinia nubilalis* (O'Connell et al. 1983; Hansson et al. 1992; Cossé et al. 1995), this arrangement seems to be rare among the heliothine species. Except for *H. assulta*, all heliothine moths studied so far have a population of relatively few neurons tuned to a behavioral antagonist, peripherally as well as centrally. Presumed that there is a certain degree of correspondence between the composition of central and peripheral neuron populations, the relatively large number of Z9-14:AL–responsive projection neurons in *H. assulta* may be related to the common principle that species of *Helicoverpa* seem to pair the Z9-16:AL- and

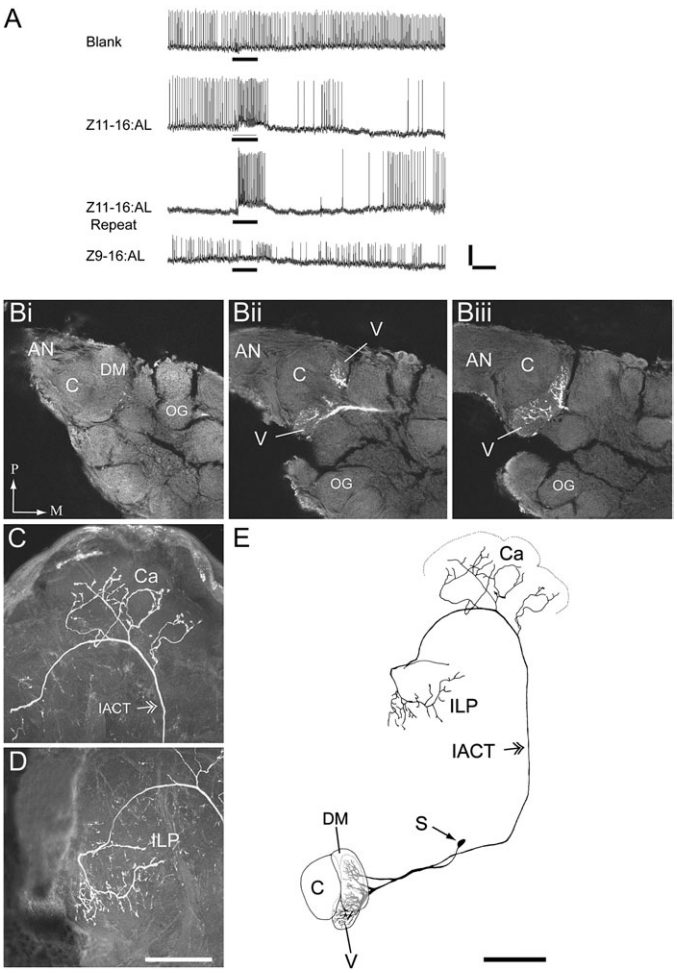

Figure 5 Physiological and morphological characteristics of a projection neuron responding to the secondary pheromone component Z11-16:AL (neuron #5). **(A)** Neuronal activity recorded during application of various stimuli to the antenna. An excitatory response to Z11-16:AL is demonstrated. Scale bars = 10 mV, 400 ms. **(Bi–Biii)** Confocal sections showing the neural arborizations in the ventral MGC unit (V) at 3 different depths (Bii 24 μm deeper than Bi; Biii 14 μm deeper than **Bii**). **(C)** Confocal reconstruction of a stack containing 58 sections (i.e., 116 μm) showing the axon (double arrow) passing in the inner antennocerebral tract (IACT) to the calyces (Ca). **(D)** Confocal reconstruction of a stack containing 66 sections (i.e., 132 μm) showing the terminals in the inferior lateral protocerebrum (ILP). **(E)** Complete reconstruction of the uniglomerular projection neuron. Scale bar = 100 μm. AN, antennal nerve; C, cumulus; DM, dorsomedial unit; OG, ordinary glomerulus; S, soma; P, posterior, M, medial.

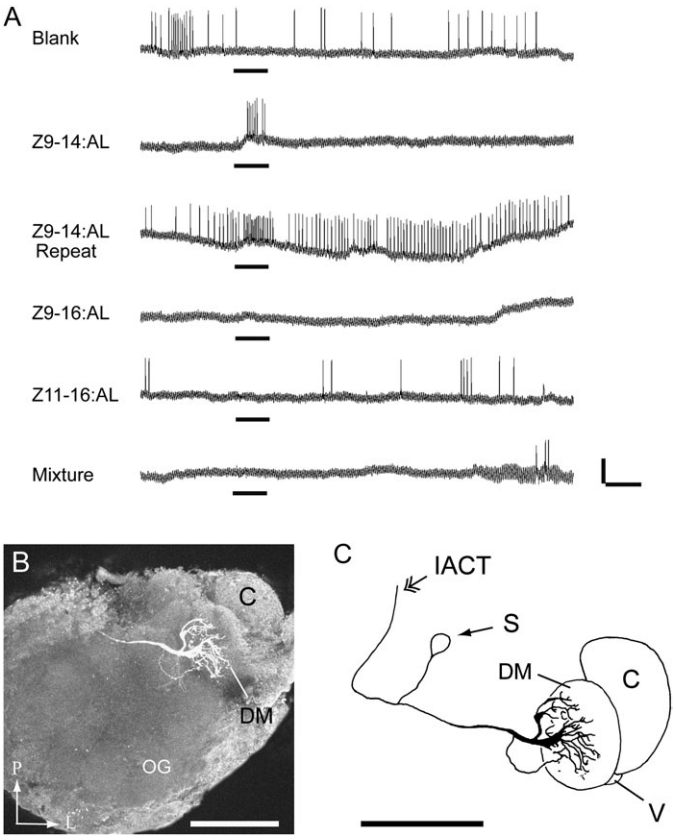

Figure 6 Physiological and morphological characteristics of a projection neuron responding to the interspecific signal Z9-14:AL (neuron #6). **(A)** Neuronal activity recorded during application of various stimuli to the antenna. An excitatory response to Z9-14:AL is demonstrated. Scale bars = 10 mV, 400 ms. **(B)** Confocal reconstruction of a stack containing 19 sections, showing neural arborizations in the dorsomedial MGC unit (DM). **(C)** Reconstruction of the neural arborizations in the DM unit. Scale bars = 100 μm. C, cumulus; OG, ordinary glomerulus, IACT, inner antennocerebral tract, S, soma; V, ventral unit; P, posterior; L, lateral.

Z9-14:AL–responsive receptor neurons (Skiri 1999; Berg et al. 2005; Lee, Vickers, and Baker 2006).

As demonstrated in the results presented here, the category of projection neurons responding to Z9-14:AL consequently arborized in the dorsomedial MGC unit. In a comparative perspective, it is noteworthy that this particular substance, being responsible for one of 2 diametrically opposite behaviors in the various species—either ensuring the male sexual behavior or interrupting this behavior—is associated with a dorsomedially located MGC unit in all species, regardless of whether the signal molecule serves as a pheromone or a behavioral antagonist (Christensen et al. 1991; Berg et al. 1998; Vickers et al. 1998). Furthermore, the Z9-14:AL–responsive receptor neurons are reported to display specific response profiles by responding second best to distinct substances in each species (Berg et al. 1995; Berg and Mustaparta 1995; Cossé et al. 1998). In general, the presence of Z9-14:AL as a biologically significant signal in intra- and interspecific communication and the diversity of physiological receptor neuron subtypes evolved for this particular substance suggest that Z9-14:AL has played an important role in speciation within this group of moths.

The secondary pheromone component Z11-16:AL is associated with the ventral MGC unit

The present finding of a Z11-16:AL–responsive projection neuron that innervates the ventral MGC unit is in

correspondence with the previous finding of a receptor neuron type activated by the same substance and with axon terminals in the same glomerulus (Berg et al. 2005). The finding of only one projection neuron of this category is also in accordance with the small number of Z11-16:AL receptor neurons previously identified in this species (Berg and Mustaparta 1995; Berg et al. 2005). The stained preparation presented here indicates a shape of the ventral MGC unit that somehow deviates from the spherical formation previously reported (Berg et al. 2002). Whether the curved shape generally characterizes the ventral MGC unit in *H. assulta* or is a peculiar finding, cannot be concluded here.

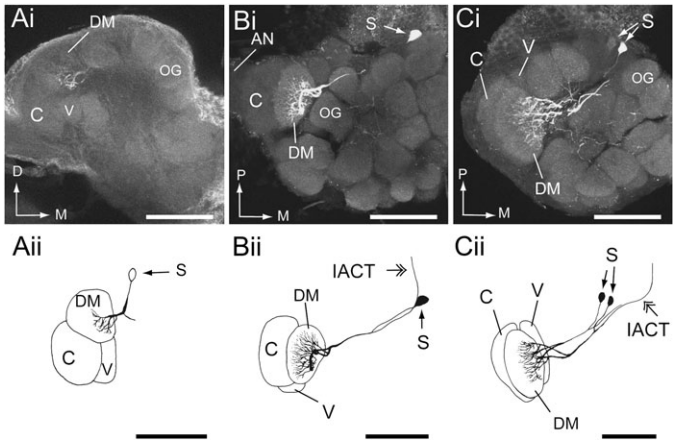

Figure 7 Confocal images and reconstructions of 3 different brain preparations, each showing a Z9-14:AL–responsive projection neurons (#7–9) arborizing in the dorsomedial MGC unit (DM). **(Ai)** Confocal reconstruction of 12 sections (i.e., 24 μm) showing dendrites in the DM unit (neuron #7). **(Aii)** Drawn reconstruction of neuron #7. **(Bi)** Confocal reconstruction of 34 sections (i.e., 68 μm) showing dense arborizations in the DM unit (neuron #8). **(Bii)** Drawn reconstruction of neuron #8. **(Ci)** Reconstruction of 34 sections (i.e., 68 μm) showing dendrites arborizing in the DM unit (neuron #9). **(Cii)** Drawn reconstruction of neuron #9. Scale bars = 100 μm. C, cumulus; V, ventral unit; OG, ordinary glomerulus; AN, antennal nerve; S, soma; IACT, inner antennocerebral tract; D, dorsal; M, medial; P, posterior.

Anatomy and physiology of the 3-unit MGC in a comparative perspective

The advantage of comparing the 2 *Helicoverpa* species, *H. assulta* and *H. armigera*, is that they utilize a binary pheromone blend consisting of the same 2 constituents in an opposite ratio and in addition an interspecific signal compound that is identical. As previously suggested by Berg et al. (2005), we may imagine how a large MGC unit tuned to Z9-16:AL and a small ventrally located MGC unit tuned to Z11-16:AL, like in *H. assulta*, can be transformed and change position during evolutionary time into a large unit tuned to Z11-16:AL and a correspondingly smaller dorsally located unit tuned to Z9-16:AL, like in *H. armigera* (and *H. zea*)—or the other way around (Figure 8). Interestingly, the 2 *Heliothis* congeners, *H. virescens* and *H. subflexa*, which are sympatric New World species utilizing the same primary pheromone component but different secondary constituents, have anatomically identical MGCs consisting of a cumulus surrounded by 3 additional glomeruli, 1 dorsomedial, and 2 ventral units (Berg et al. 1998; Vickers et al. 1998; Vickers and Christensen 2003). In this case, the species specificity is ensured by a distinct physiological tuning of the surrounding units, which means a functional divergence of spatially conserved glomeruli (Vickers and Christensen 2003). A shift of glomerular tuning in anatomically similar MGC units has also been shown in 2 pheromone strains of the European corn borer *O. nubilalis* using the same pheromone components but in opposite ratios (Kárpáti et al. 2008). The advantage of studying the 3-unit MGC of the *Helicoverpa* moths, however, is that this system may reflect how dynamic transformations of brain structures essential for speciation have evolved.

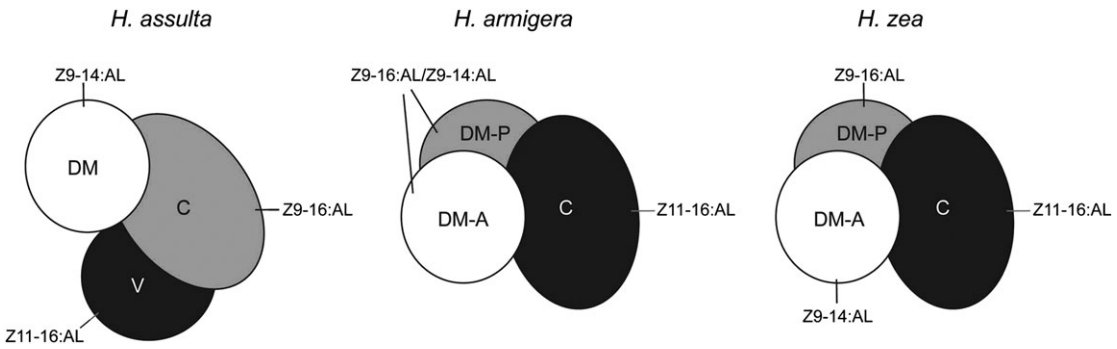

Figure 8 Schematic overview of the anatomical and functional organization of the MGC in the 3 closely related species *Helicoverpa assulta*, *H. armigera* (Skiri 1999; Skiri et al. 2005), and *H. zea* (Vickers et al. 1998; Lee, Carlsson, et al. 2006). C, cumulus; DM, dorsomedial unit; V, ventral unit. DM-A, dorsomedial anterior unit; DM-P, dorsomedial posterior unit.

Funding

Norwegian Research Council [project no 1141434].

Acknowledgements

We are grateful to Jun-Feng Dong, Henan University of Science and Technology, for regularly sending pupae. Furthermore, we thank Hanna Mustaparta, Giovanni Galizia, and Robert Brandt for allowing use of unpublished material from the previous work of Berg et al. (2002). And finally, we thank 2 anonymous reviewers for a number of constructive suggestions.

References

Anton S, Homberg U. 1999. Antennal lobe structure. In: Hansson BS, editor. Insect olfaction. Berlin (Germany): Springer. p. 97–124.

Anton S, Löfstedt C, Hansson BS. 1997. Central nervous processing of sex pheromone in two strains of the European corn borer *Ostrinia nubilalis* (Lepidoptera: Pyralidae). J Exp Biol. 200:1073–1087.

Arn H, Tooth M, Priesner E. 1992. List of sex pheromones of Lepidoptera and related attractants. 2nd ed. Wadenswill (Switzerland): IOBC–WPRS.

Baker TC, Ochieng SA, Cossé AA, Lee SG, Todd JL, Quero C, Vickers NJ. 2004. A comparison of responses from olfactory receptor neurons of *Heliothis subflexa* and *Heliothis virescens* to components of their sex pheromone. J Comp Physiol A. 190:155–165.

Berg BG, Almaas TJ, Bjaalie JG, Mustaparta H. 1998. The macroglomerular complex of the antennal lobe of tobacco budworm moth *Heliothis virescens*: specified subdivision in four compartments according to information about biologically significant compounds. J Comp Physiol A. 183:669–682.

Berg BG, Almass TJ, Bjaalie JG, Mustaparta H. 2005. Projections of male specific receptor neurons in the antennal lobe of the oriental tobacco budworm moth, Helicoverpa assulta: a unique glomerular organization among related species. J Comp Neurol. 486:209–220.

Berg BG, Galizia CG, Brandt R, Mustaparta H. 2002. Digital atlases of the antennal lobe in two species of tobacco budworm moths, the oriental *Helicoverpa assulta* (male) and the American *Heliothis virescens* (male and female). J Comp Neurol. 446:123–134.

Berg BG, Mustaparta H. 1995. The significance of major pheromone components and interspecific signals as expressed by receptor neurons in the oriental tobacco budworm moth, *Helicoverpa assulta*. J Comp Physiol A. 177:683–694.

Berg BG, Tumlinson JH, Mustaparta H. 1995. Chemical communication in heliothine moths IV. Receptor neuron responses to pheromone compounds and formate analogues in the male tobacco budworm moth *Heliothis virescens*. J Comp Physiol A. 177:527–534.

Boeckh J, Ernst KD. 1987. Contribution of single unit analysis in insects to an understanding of olfactory function. J Comp Physiol A. 161:549–565.

Boo KS, Park KC, Hall DR, Cork A, Berg BG, Mustaparta H. 1995. (Z)-9-tetradecenal: a potent inhibitor of pheromone-mediated communication in the oriental tobacco budworm moth; *Helicoverpa assulta*. J Comp Physiol A. 177:695–699.

Christensen TA, Hildebrand JG. 1987. Male specific, sex pheromone-selective projection neurons in the antennal lobes of the moth *Manduca sexta*. J Comp Physiol A. 160:553–569.

Christensen TA, Mustaparta H, Hildebrand JG. 1991. Chemical communication in heliothine moths II. Central processing of intra- and interspecific olfactory messages in the male corn earworm moth *Helicoverpa zea*. J Comp Physiol A. 169:259–274.

Christensen TA, Mustaparta H, Hildebrand JG. 1995. Chemical communication in heliothine moths. VI. Parallel pathways for information processing in the macroglomerular complex of the male tobacco budworm moth *Heliothis virescens*. J Comp Physiol A. 177: 545–557.

Cork A, Boo KS, Dunkelblom E, Hall DR, Jee-Rajunga K, Kehat M, Kong Jie E, Park KC, Tepidagarm D, Liu X. 1992. Female sex pheromone of *Helicovepa assulta* (Guenée) (Lepidoptera: Noctuidae); identification and field testing. J Chem Ecol. 18:403–418.

Cossé AA, Campbell MG, Glover TJ, Linn CE, Todd JL, Baker TC, Roelofs WL. 1995. Pheromone behavioral responses in unusual male European corn borer hybrid progeny not correlated to electrophysiological phenotypes of their pheromone-specific antennal neurons. Experientia. 51:809–816.

Cossé AA, Todd JL, Baker TC. 1998. Neurons discovered in male *Helicoverpa zea* antennae that correlate with pheromone-mediated attraction and interspecific antagonism. J Comp Physiol A. 182:585–594.

Hansson BS, Almaas TJ, Anton S. 1995. Chemical communication in heliothine moths. V. Antennal lobe projection patterns of pheromone-detecting olfactory receptor neurons in the male Heliothis virescens (Lepidoptera: Noctuidae). J Comp Physiol A. 177:535–543.

Hansson BS, Anton S, Christensen TA. 1994. Structure and function of antennal lobe neurons in the male turnip moth, *Agrotis segetum* (Lepidoptera: Noctuidae). J Comp Physiol A. 175:547–562.

Hansson BS, Christensen TA. 1999. Functional characteristics of the antennal lobe. In: Hansson BS, editor. Insect olfaction. Berlin (Germany): Springer. p. 125–161.

Hansson BS, Christensen TA, Hildebrand JG. 1991. Functionally distinct subdivisions of the macroglomerular complex in the antennal lobe of the male sphinx moth *Manduca sexta*. J Comp Neurol. 312:264–278.

Hansson BS, Ljungberg H, Hallberg E, Löfstedt C. 1992. Functional specialization of olfactory glomeruli in a moth. Science. 256:1313–1315.

Hildebrand JG, Shepherd GM. 1997. Mechanisms of olfactory discrimination: converging evidence for common principles across phyla. Annu Rev Neurosci. 20:595–631.

Homberg U, Montague RA, Hildebrand JG. 1988. Anatomy of antenna-cerebral pathways in the brain of the sphinx moth *Manduca sexta*. Cell Tissue Res. 254:255–281.

Kanzaki R, Soo K, Seki V, Wada S. 2003. Projections to higher olfactory centers from subdivisions of the antennal lobe macroglomerular complex of the male silkmoth. Chem Senses. 28:113–130.

Kárpáti Z, Dekker T, Hansson BS. 2008. Reversed functional topology in the antennal lobe of the male European corn borer. J Exp Biol. 211: 2841–2848.

Klun JA, Plimmer JR, Bierl-Leonhardt BA, Sparks AN, Primiani M, Chapman OL, Lee GH, Lepone G. 1980. Sex pheromone chemistry of female corn earworm moth, *Heliothis zea*. J Chem Ecol. 6:165–175.

Lee S-G, Carlsson MA, Hansson BS, Todd JL, Baker TC. 2006. Antennal lobe projection destinations of *Helicoverpa zea* male olfactory receptor neurons responsive to heliothine sex pheromone components. J Comp Physiol A. 192:351–363.

Lee S-G, Vickers NJ, Baker TC. 2006. Glomerular targets of *Heliothis subflexa* male olfactory receptor neurons housed within long trichoid sensilla. Chem senses. 31:821–834.

Mustaparta H. 1996. Central mechanism of pheromone information processing. Chem Senses. 21:269–275.

Ng M, Roorda RD, Lima SQ, Zemelman BV, Morcillo P, Miesenböck G. 2002. Transmission of olfactory information between three populations of neurons in the antennal lobe of the fly. Neuron. 36:463–474.

O'Connell RJ, Grant AJ, Mayer MS, Mankin RW. 1983. Morphological correlates of differences in pheromone sensitivity in insect sensilla. Science. 220:1408–1410.

Park KC, Cork A, Boo KS, Hall DR. 1994. Biological activity of female sex pheromone of the oriental tobacco budworm moth, *Helicoverpa assulta* (Guenée) (Lepidoptera: Noctuidae), electroantennography, wind tunnel observations and field trapping. Korean J Appl Entomol. 33:26–32.

Root CM, Semmelhack JL, Wong AM, Flores J, Wang JW. 2007. Propagation of olfactory information in *Drosophila*. Proc Natl Acad Sci U S A. 104: 11826–11831.

Skiri HT. 1999. Funksjonell organisering av makroglomerularkomplekset i antenneloben hos nattsvermerarten *Helicoverpa armigera* [MSc thesis]. [Trondheim (Norway)]: Norwegian University of Science and Technology.

Skiri HT, Rø H, Berg BG, Mustaparta H. 2005. Consistent organization of glomeruli in the antennal lobes of related species of heliothine moths. J Comp Neurol. 491:367–380.

Stranden M, Røstelien T, Liblikas I, Almaas TJ, Borg-Karlson A-K, Mustaparta H. 2003. Receptor neurones in three heliothine moths responding to floral and inducible plant volatiles. Chemoecology. 13: 143–154.

Sugie H, Tatsuki S, Nakagaki S, Bao CBJ, Yamamoto A. 1991. Identification of sex pheromone of the oriental tobacco budworm moth, *Heliothis assulta* (Guenée) (Lepidoptera: Noctuidae). Appl Entomol Zool. 26:151–153.

Vickers NJ, Christensen TA. 2003. Functional divergence of spatially conserved olfactory glomeruli in two related moth species. Chem Senses. 28:325–338.

Vickers NJ, Christensen TA, Hildebrand JG. 1998. Combinatorial odor discrimination in the brain: attractive and antagonist odor blends are represented in distinct combination of uniquely identifiable glomeruli. J Comp Neurol. 400:35–56.

Wang H-L, Zhao C-H, Wang C-Z. 2005. Comparative study of sex pheromone composition and biosynthesis in *Helicoverpa armigera, H. assulta* and their hybrid. Insect Biochem Mol Biol. 35:575–583.

Wilson RI, Turner GC, Laurent G. 2004. Transformation of olfactory representations in the *Drosophila* antennal lobe. Science. 303:366–370.

Zhao XC, Berg BG. 2009. Morphological and physiological characteristics of the serotonin-immunoreactive neuron in the antennal lobe of the male oriental tobacco budworm, *Helicoverpa assulta*. Chem Senses. 34: 363–372.